1 **Contribution of structural recalcitrance to the formation of the deep**

2 **oceanic dissolved organic carbon reservoir**

3

4 Nannan Wang[1,2], Ya-Wei Luo[2], Luca Polimene[3], Rui Zhang[2], Qiang Zheng[2],

5 Ruanhong Cai[2], Nianzhi Jiao[2*]

6

7 [1] College of Environment and Ecology, Xiamen University, Xiamen 361102, China.

8 [2] State Key Laboratory of Marine Environmental Sciences, Xiamen University,

9 Xiamen 361102, China.

10 [3]Plymouth Marine Laboratory, Prospect Place, The Hoe, Plymouth, UK.

11

12 Running title: Structural recalcitrance dominates DOM persistence

13

14 Correspondence: *Nianzhi Jiao; Address: Zhoulongquan BLDG, Xiangan South Road,

15 Xiamen, Fujian 361102, China; E-mail: jiao@xmu.edu.cn; Tel.: 86-592-2880199; Fax:

16 86-592-2880150.

Originality-Significance Statement

There is a lively debate over why the large recalcitrant dissolved organic carbon (DOC) reservoir persists in the ocean for extended time periods (up to millennia). Here, we evaluate the relative contributions of structurally recalcitrant DOC and recalcitrant DOC due to dilution to deep oceanic DOC pool by modeling transformations of the different DOC components in incubation experiments with different DOC concentration levels. We conclude that the majority of DOC in the deep ocean is structurally recalcitrant, which supports the hypothesis that the recalcitrance of RDOC is largely related to its chemical properties rather than its low concentration. This also implies that recalcitrant DOC is independent of from RDOC concentration threshold for bacterial uptake.

Summary

The origin of the recalcitrant dissolved organic carbon (RDOC) reservoir in the deep ocean remains enigmatic. The structural recalcitrance hypothesis suggests that RDOC is formed by molecules that are chemically resistant to bacterial degradation. The dilution hypothesis claims that RDOC is formed from a large diversity of labile molecules that escape bacterial utilization due to their low concentrations, termed as $RDOC_c$. To evaluate the relative contributions of these two mechanisms in determining the long-term persistence of RDOC, we model the dynamics of both structurally recalcitrant DOC and $RDOC_c$ based on previously published data that describes deep oceanic DOC degradation experiments. Our results demonstrate that the majority DOC ($84.5\pm2.2\%$) in the deep ocean is structurally recalcitrant. The intrinsically labile DOC (i.e., labile DOC that rapidly consumed and $RDOC_c$) accounts for a relatively small proportion and is consumed rapidly in the incubation experiments, in which $47.8\pm3.2\%$ of labile DOC and $21.9\pm4.6\%$ of $RDOC_c$ is consumed in 40 days. Our results suggest that the recalcitrance of RDOC is largely related to its chemical properties, whereas dilution plays a minor role in determining the persistence of deep-ocean DOC.

Introduction

The ocean contains a large amount of recalcitrant dissolved organic carbon (RDOC). This reservoir plays a critical role in global carbon sequestration and potentially affects global climate (Hansell et al., 2009; Jiao et al., 2014). Although we know that RDOC persists in the water column for thousands of years (Brophy and Carlson, 1989; Lancelot et al., 1993; Carlson and Ducklow, 1995; Jiao et al., 2010; Hansell, 2013), the mechanisms underpinning this extraordinary stability remain objects of controversy (Arrieta et al., 2015b, a; Jiao et al., 2015).

Two primary but not mutually exclusive mechanisms have been proposed to explain the persistence of RDOC. The dilution hypothesis postulates that the deep oceanic dissolved organic carbon (DOC) consists of a large diversity of extremely diluted molecules, termed $RDOC_c$. These molecules, although chemically labile, would not be consumed by bacteria because their concentrations could be below the thresholds for direct assimilatory uptake and the metabolic requirements for their degradation cannot be satisfied (Jannasch, 1967; Barber, 1968; Dittmar and Paeng, 2009; Kujawinski, 2011; Arrieta et al., 2015b, a). This hypothesis is supported by experimental observations showing that the growth of microbes ceased if their substrates fell below a defined concentration threshold (Jannasch, 1967, 1994; Martens-Habbena et al., 2009; Arrieta et al., 2015b, a).

Another explanation for the long-term persistence of RDOC is the structural recalcitrance of the molecules in a specific environmental context, which corresponds to the previously proposed concept of biologically inert RDOC ($RDOC_t$) (Jiao et al., 2014). This idea is supported by the evidence that the chemical composition of the DOC in the deep ocean, where the RDOC dominates, is different from that of

69   decomposable DOC (Jannasch, 1967; Lancelot et al., 1993; Kaiser and Benner, 2009;

70   Jiao et al., 2010; Benner and Amon, 2015; Walker et al., 2016b). Indeed, solid phase

71   extracted (SPE) DOC from deep ocean generally features higher double-bond

72   equivalent values, lower O/C and H/C ratios, as well as a higher degree of

73   unsaturation and rings in molecules, than that from surface waters (Koch et al., 2005;

74   Flerus et al., 2012; Koch et al., 2014; Hansman et al., 2015; Arakawa et al., 2017; Jiao

75   et al., 2018). Although a complete chemical characterization of marine DOM is

76   currently lacking, it was reported that RDOC produced from bacterial consumption of

77   simple substrates contains carboxyl and fused alicyclic functional groups, which

78   determines its resistance to biodegradation and refractory nature (Ogawa et al., 2001;

79   Hertkorn et al., 2006; Lechtenfeld et al., 2014). For instance, the carboxyl-rich

80   alicyclic molecules (CRAM), which account for ~8% of the DOC, are one of the most

81   abundant organic components ever identified in the deep ocean (Hertkorn et al., 2006;

82   Hertkorn et al., 2012; Lechtenfeld et al., 2015; Rossel et al., 2015).

83   Both $RDOC_c$ and $RDOC_t$ are products of the microbial carbon pump (MCP) since

84   they are gradually generated by the successive and repetitive actions of bacteria

85   degrading relatively more labile substrates (Jiao et al., 2014). However, the

86   implications that these two pools have for the capacity of the MCP to store carbon by

87   forming RDOC differ dramatically. If the majority of RDOC is $RDOC_c$, the capacity

88   of the ocean to store carbon as RDOC would be limited by the DOC concentration

89   threshold for bacterial uptake (i.e., RDOC cannot exceed that threshold otherwise it is

90   consumed by microbes). In contrast, if the majority of RDOC is $RDOC_t$, the capacity

91   of the ocean to store carbon via the MCP would be independent from RDOC

92   concentrations. Therefore, the trade-off between these two forms of recalcitrance

93   would profoundly influence the capacity of the ocean to store carbon as RDOC and

94   thus influence the impacts of ocean carbon dynamics on climate change.

95   In this study, we assess the relative contributions of the dilution and structural

96   recalcitrance hypotheses in determining the long-term persistence of DOC by

97   reanalyzing published data from a DOC degradation experiment (Arrieta et al.,

98   2015b), in which natural bacterial communities from the deep Pacific and Atlantic

99   oceans were incubated with deep-water SPE DOC at different concentrations in about

100   40 days. The dataset includes measurements of SPE DOC utilization and Fourier

101   transform ion cyclotron resonance mass spectrometry (FT-ICR-MS) data of

102   hydrophobic SPE DOM (~40% of total seawater DOC). Although the FT-ICR-MS is

103   not totally quantitative due to the matrix effect (i.e., matrix-dependent ion

104   suppression), appropriate standardization and experimental designs allow us to

105   identify molecules that are consumed or produced (Arrieta et al., 2015a) and

106   investigate the influence of the matrix effect on results (Osterholz et al., 2015). Here,

107   we model the dynamics of DOC components under the framework that i) the initial

108   deep oceanic DOC is composed of structurally recalcitrant DOC ($RDOC_t$),

109   biodegradable DOC with extremely low individual concentrations that are below the

110   corresponding microbial uptake thresholds ($RDOC_c$) and labile DOC ready for

111   microbial utilization (LDOC); and ii) LDOC is utilized in both controls and

112   concentrated treatments, while $RDOC_c$ can only be partially utilized in concentrated

113   treatments (**Figure 1**). By leveraging the FT-ICR-MS profiling, which characterizes

114   SPE DOM molecular composition changes, we define a utilization index for each

115   compound by comparing the relative intensity of normalized FT-ICR-MS signal at the

116   start and at the end of the experiments. Then, we calculate the proportion of

117   intrinsically labile DOC (LDOC and $RDOC_c$) consumed by averaging the utilization

118 index of compounds that are significantly utilized. Ultimately, the contributions of

119 $RDOC_c$ and $RDOC_t$ to the deep oceanic DOC pool are quantified by comparing the

120 observed SPE DOC consumption to the consumption of the intrinsically labile DOC

121 with constraints on the DOC production process.

122

Results and Discussion

123

The intrinsically labile DOC was rapidly utilized

124

125 We first estimate the percentage of consumed intrinsically labile DOC in relation to

126 initial intrinsically labile DOC (c_l for LDOC and c_c for $RDOC_c$ as shown in **Table 1**)

127 based on significantly utilized molecules. The percentage of LDOC consumed are

128 estimated to be 54.9±3.3% and 47.8±3.2% for experiments O and P respectively

129 (**Table 2**), meaning that approximately half of the LDOC was consumed in the 40-day

130 incubation. This indicates that the intrinsically labile DOC was quickly consumed,

131 which is consistent with the observations from recent bioassay experiments that

132 approximately 75% of labile DOC was consumed in less than 30 days (Lechtenfeld et

133 al., 2015) and supports labile DOC cycles with timescales of days to weeks (Benner

134 and Amon, 2015; Hansman et al., 2015). The propagation uncertainty caused by

135 measurement variability is approximately one order of magnitude lower than the

136 estimates, allowing us to rule out measurement uncertainty caused by the FT-ICR-MS

137 data.

138 The additional removal of deep oceanic DOC, i.e., $RDOC_c$ could be observed within

139 concentrated treatments by comparing the normalized FT-ICR-MS signals at the end

140 of controls and 5-fold concentrated treatments. It shows that approximately 25% of

141 compounds in the $RDOC_c$ pool has been utilized, i.e., 25.2±3.4% for station O and

142 21.9±4.6% for station P (**Table 2**). Together with the evidence of microbial growth

143 data shown in Arrieta et al. (2015a), it supports the existence of $RDOC_c$ in the deep

144 ocean. The percentage of $RDOC_c$ consumed (21.9% to 25.2%) is smaller than that of

145 LDOC (47.8% to 54.9%), which can be attributed to the fact that molecules from the

146 $RDOC_c$ pool are too diluted and have less chance to be encountered by microbes for

147 consumption (Hansell and Carlson, 2014). Analogous to the estimates of c_l with

148 narrow ranges of propagation uncertainty, the propagation of measurement

149 uncertainty on c_c is lower than 4.6% as well (**Table 2**). Notably, our method provides

150 the lower limits of c_l and c_c rather than their true values (see **Supplementary**

151 **Methods**), implying that there would be more intrinsically labile DOC consumed in

152 reality than in our estimates.

The majority of deep oceanic DOC is $RDOC_t$

154 The observed percentage of SPE DOC consumed (i.e., c_{1X} and c_{5X}) in the incubation

155 periods are 2.1% and 4.1% for controls and 5-fold concentrated treatments,

156 respectively (**Table 3**; **Supplementary Methods**). The percentage of $RDOC_t$ in SPE

157 DOC is estimated from equation (8) in Methods. Taking results from experiment O as

158 an example (**Table 2**), LDOC and $RDOC_c$ account for less than 4.4% and 9.1% of

159 SPE DOC, respectively, which implies that $RDOC_t$ represents up to 86.6±1.2% of

160 SPE DOC. The extensive sensitivity tests show that even using a very wide range of

161 parameter values (**Table 3**), the estimate of the percentage of $RDOC_t$ in SPE DOC

162 changes no more than 2.3%, except for the effect of c_{5X} that yields no more than 9.0%

163 of the change. Therefore, our results are robust with respect to the choice of

164 parameters. Repeating the same model process on the dataset from experiment P

165 shows similar results in which the percentage of $RDOC_t$ in SPE DOC is estimated to

166 be 84.5±2.2%. Based on these results, we propose that the majority of the SPE DOC

167 is recalcitrant due to its structurally recalcitrant property rather than the dilution.

168 Since FT-ICR-MS data only provide molecular formulas and no chemical structures,

169 it is impossible to unambiguously designate a specific compound as being refractory

170 due to dilution or chemical structure without any experimental treatments. Here, we

171 have reanalyzed FT-ICR-MS datasets from substrate utilization experiments with

172 concentrated treatments and explored the contributions of both $RDOC_c$ and $RDOC_t$ to

173 long-term persistence of RDOC in the deep ocean. The key rationale of our method is

174 that a fraction of $RDOC_c$ becomes bioavailable when increasing the DOC

175 concentrations, the process of which allows the differentiation between compounds

176 with low concentration (i.e., $RDOC_c$) and structurally recalcitrant compounds (i.e.,

177 $RDOC_t$) in each mass peak and thus the quantification of their respective

178 contributions to the peak magnitude. One caveat to use the FT-ICR-MS data is that the

179 efficiency of the SPE method (Bond-Elut-PPL, 1g) is ~40% as shown in Arrieta et al.

180 (2015a) and possibly introduces compositional bias towards hydrophobic compounds

181 while losing other DOC compounds (Coppola et al., 2015; Broek et al., 2017).

182 However, it is shown that the radiocarbon ($\Delta^{14}C$) values and C/N ratios of PPL SPE

183 DOC are statistically indistinguishable from those of bulk DOC at depth, which

184 suggests that PPL SPE DOC is a close representative of the deep oceanic DOC

185 dominated by refractory compounds (Broek et al., 2017). Considering the extracted

186 DOC in experiments O and P are from deep ocean, we could ignore the influence of

187 compositional bias caused by the PPL extraction and generalize our conclusion that

188 $RDOC_t$ dominates the deep oceanic DOC. Matrix-dependent ion suppression is

189 another issue related to the use of FT-ICR-MS data (Trufelli et al., 2011; Osterholz et

190 al., 2015). In the enrichment experiments, incubation and DOC concentrated

191 treatments can result in the changes of both DOC composition and concentration, and

192 therefore lead to the matrix effect. Our model considers matrix-dependent ion

193 suppression to be an inherent assumption, and we evaluate the matrix effect caused by

194 DOC composition and concentration changes in incubation experiments (**Figure S2**).

195 When matrix effect is considered, $RDOC_t$ accounts for 82.1~89.1% and 77.8~87.9%

196 of SPE DOC for experiments O and P, respectively (**Table S1**), showing that the

197 matrix effect is unlikely to affect our estimates. However, considering that the matrix

198 effect is a complex issue with poorly understood mechanisms, we should pay a great

199 attention to sample preparation and the use of calibration approach for the FT-ICR-

200 MS community in publishing future datasets (Trufelli, et al., 2010).

201 Our results are consistent with the size-reactivity model and other studies that link the

202 radiocarbon age of organic matter to its chemical composition (Loh et al., 2004;

203 Repeta and Aluwihare, 2006; Walker et al., 2014; Benner and Amon, 2015; Walker et

204 al., 2016a; Walker et al., 2016b). The size-age-composition relationship that organic

205 matter size is negatively correlated with radiocarbon age and carbon:nitrogen ratios

206 supports the dominant role of chemical composition in determining the recalcitrance

207 of the RDOC pool (Walker et al., 2016b). In addition, if the majority of deep oceanic

208 DOC is $RDOC_c$, deep ocean $\Delta^{14}C$ calculated from the mass balance model would be

209 difficult to reconcile with its observation (Wilson and Arndt, 2017). Most recently, an

210 experimental study using large volume water column (>100 tons) shows that the

211 microbial transformation of LDOC to RDOC in a standing ecosystem can be

212 completed in a very short time (a few months) (Jiao et al., 2018), providing further

213 evidence for the dominance of $RDOC_t$.

It is worth noting that the study of Arrieta et al. (2015a) also refers to the $RDOC_c$ fraction by constructing a utilization index of the relative abundance of molecules, which showed that there are more than 70% and 40% of DOC is $RDOC_c$ in the deep ocean for experiments O and P, respectively, i.e., no more than 30% and 60% of DOC is $RDOC_t$. This discrepancy from our study can be attributed to different assumptions in the estimation. Their estimation assumes that each molecule is either intrinsically labile or structurally recalcitrant. Therefore the significantly utilized molecules detected by utilization index are only intrinsically labile, i.e., LDOC and $RDOC_c$. However, our method assumes that each observed peak likely contains both intrinsically labile DOC and $RDOC_t$ components, since that the structural isomers with different bioavailability cannot be distinguished with the limit of current FT-ICR MS technology (Stubbins et al., 2014; Osterholz et al., 2015).

Explanations of low DOC consumption in concentrated experiments

Arrieta and coworkers have stated that the 'dilution hypothesis is the primary mechanism controlling on the biogeochemical cycling of DOC in the deep ocean' (Arrieta et al., 2015b). It has been pointed out that there is no significant increase in DOC consumption (<6%) when increasing DOC concentrations (Jiao et al., 2015). Arrieta and coworkers explained that it would take a longer time for complete consumption of labile substrates and illustrated this process by a simulation study that assumed that DOC utilization depends only on concentration. Here, we carry out a similar simulation but under a more general case that deep oceanic DOC is a mixture of structurally recalcitrant and intrinsically labile DOC. If no $RDOC_t$ is available in the original SPE DOC (**Figure 2A**), the simulation results are equal to those reported in Arrieta et al. (Arrieta et al., 2015a). The SPE DOC utilized after 40 days is 2.1±0.7%, 2.6±0.9%, 3.7±1.2% and 5.2±1.7% of the initial concentrations for controls,

239 2-, 5-, and 10-fold concentrated treatments, respectively. However, if the percentage

240 of RDOC$_t$ in total DOC varies from 10% to 90% (**Figure 2B-D**), there is no apparent

241 difference in DOC consumption rate among the four scenarios at the 40-day time

242 scale. Based on our conservative estimate of the percentage of RDOC$_t$ in total DOC

243 (84.5%), the DOC utilized after 40 days would be 2.1±0.7%, 2.5±0.8%, 3.5±1.1% and

244 4.8±1.5% of the initial concentration for controls and concentrated treatments, which

245 are still well within the range of the observations (<6%) and have slight difference

246 from those estimated under the assumption that no RDOC$_t$ exists.

247 Till now, there are two plausible interpretations about the low DOC consumption in

248 enrichment experiments. The first one, illustrated in Arrieta et al. (2015a),

249 hypothesizes that a large fraction of DOC in the deep ocean is intrinsically labile

250 compounds and attributes the low DOC consumption even under concentrated

251 treatments to the short-term incubation. In other words, the concentrated DOC could

252 be completely consumed if given longer time for incubation (**Figure 3A**). In contrast,

253 our results show that the percentage of intrinsically labile DOC consumed is high in

254 less than 40-days of incubation (>47.8% for LDOC and >21.9% for RDOC$_c$), but the

255 small fraction of intrinsically labile DOC results in the small bulk DOC consumption

256 (**Figure 3B**). Interestingly, this discussion is also consistent with the results obtained

257 by a different modeling approach that explored the radiocarbon signature of DOC in

258 relation to the dilution theory (Wilson and Arndt, 2017). While both the models

259 suggest that DOC recalcitrance is largely related to its chemical composition, they

260 also imply that RDOC$_c$ plays a secondary role in explaining the long-term persistence

261 of deep oceanic DOC.

262 **Conclusions**

263   In summary, our results support the hypothesis that RDOC in the deep ocean is

264   dominated by structurally recalcitrant $RDOC_t$, i.e. at least 84.5% of RDOC in this

265   case. The LDOC and $RDOC_c$ account for a relatively minor fraction of the bulk

266   RDOC (<5.0% for LDOC and <10.5% for $RDOC_c$) and can be rapidly used. The high

267   proportion of $RDOC_t$ implies that the capacity of the ocean to store carbon via MCP is

268   not constrained by a dilution threshold. Further investigations are required to

269   understand if the current pool of oceanic RDOC could increase, potentially

270   counteracting the anthropogenically induced increase in atmospheric CO_2.

Conflict of interest

280   All authors have seen and approved the final version submitted, and declared no

281   conflict of interest.

Supporting Information

283   Additional Supporting Information may be found in the online version of this article.

284   **Supplementary Methods.** Descriptive information regarding the methods used

285   within this study.

Supplementary Tables and Figures

Table S1. Matrix effect on estimating the percentage of RDOC$_t$ in SPE DOC (f_t). Here, we consider the matrix effect caused by the incubation process (i.e., change of signal intensity from DOC component during incubation experiments) and concentrated treatments (i.e., change of signal intensity due to DOC concentrated treatments). The measurement uncertainty caused by matrix effect (i.e., σ_{ME}) is calculated as the 95th percentile of signal intensity difference by comparing 1X initial and 1X final FT-ICR-MS, 1X initial and 5X initial FT-ICR-MS, 5X initial and 5X final FT-ICR-MS, respectively. We then investigate the matrix effect on the estimation of f_t according to equation (17) in Supplementary Methods.

Figure S1. Histogram distribution of measurement variability of FT-ICR-MS fingerprints of DOC by assembling all molecules together. The measurement variability for each molecule is calculated as the standard deviation of its relative intensities from replicates. The average measurement variability FT-ICR-MS (i.e., σ_m) is chosen as the 95th percentile of this distribution for the downstream propagation uncertainty analysis.

Figure S2. Comparison of signal intensity of FT-ICR-MS to assess DOC composition change during the incubation experiments (A, B, D, E) and the matrix effect due to DOC concentrated treatments (C, F). The diagonal line is shown in the red color in each figure.

.
References

Arakawa, N., Aluwihare, L.I., Simpson, A.J., Soong, R., Stephens, B.M., and Lane-Coplen, D. (2017) Carotenoids are the likely precursor of a significant fraction of marine dissolved organic matter. *Science advances* **3**: e1602976.

Arrieta, J.M., Mayol, E., Hansman, R.L., Herndl, G.J., Dittmar, T., and Duarte, C.M. (2015a) Response to Comment on "Dilution limits dissolved organic carbon utilization in the deep ocean". *Science* **350**: 1483-1483.

Arrieta, J.M., Mayol, E., Hansman, R.L., Herndl, G.J., Dittmar, T., and Duarte, C.M. (2015b) Dilution

315   limits dissolved organic carbon utilization in the deep ocean. *Science* **348**: 331-333.

316 Barber, R.T. (1968) Dissolved organic carbon from deep waters resists microbial oxidation.
317   *Nature* **220**: 274-275.

318 Benner, R., and Amon, R.M. (2015) The size-reactivity continuum of major bioelements in the
319   ocean. *Annual review of marine science* **7**: 185-205.

320 Broek, T.A., Walker, B.D., Guilderson, T.P., and McCarthy, M.D. (2017) Coupled ultrafiltration and
321   solid phase extraction approach for the targeted study of semi-labile high molecular weight
322   and refractory low molecular weight dissolved organic matter. *Marine Chemistry* **194**: 146-
323   157.

324 Brophy, J.E., and Carlson, D.J. (1989) Production of biologically refractory dissolved organic
325   carbon by natural seawater microbial populations. *Deep Sea Research Part A Oceanographic*
326   *Research Papers* **36**: 497-507.

327 Carlson, C., and Ducklow, H. (1995) Dissolved organic carbon in the upper ocean of the central
328   equatorial Pacific Ocean, 1992: Daily and finescale vertical variations. *Deep Sea Research Part*
329   *II: Topical Studies in Oceanography* **42**: 639-656.

330 Coppola, A.I., Walker, B.D., and Druffel, E.R. (2015) Solid phase extraction method for the study of
331   black carbon cycling in dissolved organic carbon using radiocarbon. *Marine Chemistry* **177**:
332   697-705.

333 Dittmar, T., and Paeng, J. (2009) A heat-induced molecular signature in marine dissolved organic
334   matter. *Nature Geoscience* **2**: 175.

335 Flerus, R., Lechtenfeld, O., Koch, B.P., McCallister, S., Schmitt-Kopplin, P., Benner, R. et al. (2012) A
336   molecular perspective on the ageing of marine dissolved organic matter. *Biogeosciences* **9**:
337   1935.

338 Hansell, D.A. (2013) Recalcitrant dissolved organic carbon fractions.

339 Hansell, D.A., and Carlson, C.A. (2014) *Biogeochemistry of marine dissolved organic matter*:
340   Academic Press.

341 Hansell, D.A., Carlson, C.A., Repeta, D.J., and Schlitzer, R. (2009) Dissolved organic matter in the
342   ocean: A controversy stimulates new insights. *Oceanography* **22**: 202-211.

343 Hansman, R.L., Dittmar, T., and Herndl, G.J. (2015) Conservation of dissolved organic matter
344   molecular composition during mixing of the deep water masses of the northeast Atlantic
345   Ocean. *Marine Chemistry* **177**: 288-297.

346 Hertkorn, N., Harir, M., Koch, B., Michalke, B., Grill, P., and Schmitt-Kopplin, P. (2012) High field
347   NMR spectroscopy and FTICR mass spectrometry: powerful discovery tools for the molecular
348   level characterization of marine dissolved organic matter from the South Atlantic Ocean.
349   *Biogeosciences Discussions* **9**.

350 Hertkorn, N., Benner, R., Frommberger, M., Schmitt-Kopplin, P., Witt, M., Kaiser, K. et al. (2006)
351   Characterization of a major refractory component of marine dissolved organic matter.
352   *Geochimica et Cosmochimica Acta* **70**: 2990-3010.

353 Jannasch, H.W. (1967) Growth of marine bacteria at limiting concentrations of organic carbon in
354   seawater. *Limnology and Oceanography* **12**: 264-271.

355 Jannasch, H.W. (1994) The microbial turnover of carbon in the deep-sea environment. *Global and*
356   *Planetary Change* **9**: 289-295.

357 Jiao, N., Herndl, G.J., Hansell, D.A., Benner, R., Kattner, G., Wilhelm, S.W. et al. (2010) Microbial
358   production of recalcitrant dissolved organic matter: long-term carbon storage in the global
359   ocean. *Nature reviews Microbiology* **8**: 593.

360 Jiao, N., Robinson, C., Azam, F., Thomas, H., Baltar, F., Dang, H. et al. (2014) Mechanisms of
361   microbial carbon sequestration in the ocean–future research directions. *Biogeosciences* **11**:
362   5285-5306.

363 Jiao, N., Legendre, L., Robinson, C., Thomas, H., Luo, Y.-W., Dang, H. et al. (2015) Comment on

364   "Dilution limits dissolved organic carbon utilization in the deep ocean". *Science* **350**: 1483-
365   1483.

366   Jiao, N., Cai, R., Zheng, Q., Tang, K., Liu, J., Jiao, F. et al. (2018) Unveiling the enigma of refractory
367   carbon in the ocean. *National Science Review*.

368   Kaiser, K., and Benner, R. (2009) Biochemical composition and size distribution of organic matter
369   at the Pacific and Atlantic time-series stations. *Marine Chemistry* **113**: 63-77.

370   Koch, B., Kattner, G., Witt, M., and Passow, U. (2014) Molecular insights into the microbial
371   formation of marine dissolved organic matter: recalcitrant or labile? *Biogeosciences* **11**: 4173-
372   4190.

373   Koch, B.P., Witt, M., Engbrodt, R., Dittmar, T., and Kattner, G. (2005) Molecular formulae of marine
374   and terrigenous dissolved organic matter detected by electrospray ionization Fourier
375   transform ion cyclotron resonance mass spectrometry. *Geochimica et Cosmochimica Acta* **69**:
376   3299-3308.

377   Kujawinski, E.B. (2011) The impact of microbial metabolism on marine dissolved organic matter.
378   *Annual review of marine science* **3**: 567-599.

379   Lancelot, C., Fasham, M., Legendre, L., Radach, G., Scott, M., and Kirchman, D.L. (1993) Dissolved
380   organic matter in biogeochemical models of the ocean. In *Towards a model of ocean
381   biogeochemical processes*: Springer, pp. 209-225.

382   Lechtenfeld, O.J., Hertkorn, N., Shen, Y., Witt, M., and Benner, R. (2015) Marine sequestration of
383   carbon in bacterial metabolites. *Nature communications* **6**: 6711.

384   Lechtenfeld, O.J., Kattner, G., Flerus, R., McCallister, S.L., Schmitt-Kopplin, P., and Koch, B.P. (2014)
385   Molecular transformation and degradation of refractory dissolved organic matter in the
386   Atlantic and Southern Ocean. *Geochimica et Cosmochimica Acta* **126**: 321-337.

387   Loh, A.N., Bauer, J.E., and Druffel, E.R. (2004) Variable ageing and storage of dissolved organic
388   components in the open ocean. *Nature* **430**: 877.

389   Martens-Habbena, W., Berube, P.M., Urakawa, H., de La Torre, J.R., and Stahl, D.A. (2009) Ammonia
390   oxidation kinetics determine niche separation of nitrifying Archaea and Bacteria. *Nature* **461**:
391   976.

392   Ogawa, H., Amagai, Y., Koike, I., Kaiser, K., and Benner, R. (2001) Production of refractory dissolved
393   organic matter by bacteria. *Science* **292**: 917-920.

394   Osterholz, H., Niggemann, J., Giebel, H.-A., Simon, M., and Dittmar, T. (2015) Inefficient microbial
395   production of refractory dissolved organic matter in the ocean. *Nature communications* **6**:
396   7422.

397   Repeta, D.J., and Aluwihare, L.I. (2006) Radiocarbon analysis of neutral sugars in high‐molecular
398   ‐weight dissolved organic carbon: Implications for organic carbon cycling. *Limnology and
399   Oceanography* **51**: 1045-1053.

400   Rossel, P.E., Stubbins, A., Hach, P.F., and Dittmar, T. (2015) Bioavailability and molecular
401   composition of dissolved organic matter from a diffuse hydrothermal system. *Marine
402   Chemistry* **177**: 257-266.

403   Stoderegger, K., and Herndl, G.J. (1998) Production and release of bacterial capsular material and
404   its subsequent utilization by marine bacterioplankton. *Limnology and Oceanography* **43**: 877-
405   884.

406   Stubbins, A., Lapierre, J.-F., Berggren, M., Prairie, Y.T., Dittmar, T., and del Giorgio, P.A. (2014)
407   What's in an EEM? Molecular signatures associated with dissolved organic fluorescence in
408   boreal Canada. *Environmental science & technology* **48**: 10598-10606.

409   Trufelli, H., Palma, P., Famiglini, G., and Cappiello, A. (2011) An overview of matrix effects in liquid
410   chromatography–mass spectrometry. *Mass spectrometry reviews* **30**: 491-509.

411   Walker, B., Guilderson, T., Okimura, K., Peacock, M., and McCarthy, M. (2014) Radiocarbon
412   signatures and size–age–composition relationships of major organic matter pools within a

413   unique California upwelling system. *Geochimica et Cosmochimica Acta* **126**: 1-17.

414   Walker, B., Primeau, F., Beaupré, S., Guilderson, T., Druffel, E., and McCarthy, M. (2016a) Linked
415   changes in marine dissolved organic carbon molecular size and radiocarbon age. *Geophysical*
416   *Research Letters* **43**.

417   Walker, B.D., Beaupré, S.R., Guilderson, T.P., McCarthy, M.D., and Druffel, E.R. (2016b) Pacific
418   carbon cycling constrained by organic matter size, age and composition relationships. *Nature*
419   *Geoscience* **9**.

420   Wilson, J.D., and Arndt, S. (2017) Modeling radiocarbon constraints on the dilution of dissolved
421   organic carbon in the deep ocean. *Global Biogeochemical Cycles.*

422

Tables

Table 1. Model parameters with their indicators. All are unitless.

Meaning	Symbol	Standard value	Source
The percentage of RDOC$_t$ in SPE DOC pool	f_t	-	-
The percentage of RDOC$_c$ in SPE DOC pool	f_c	-	-
The percentage of LDOC in SPE DOC pool	f_l	-	-
The percentage of consumed RDOC$_c$ in relation to initial RDOC$_c$	c_c	-	-
The percentage of consumed LDOC in relation to initial LDOC	c_l	-	-
The percentage of consumed DOC in relation to SPE DOC in controls	c_{1X}	2.1%	Arrieta et al. (2015a)
The percentage of consumed DOC in relation to SPE DOC in 5-fold concentrated treatments	c_{5X}	4.1%	Arrieta et al. (2015a)
The new DOC produced per unit of LDOC consumed	p_l	12.5%	(Stoderegger and Herndl, 1998)
The new DOC produced per unit of RDOC$_c$ consumed	p_c	12.5%	(Stoderegger and Herndl, 1998)

429 **Table 2.** Propagation of measurement uncertainty of FT-ICR-MS on estimating the

430 percentage of RDOC$_t$ in SPE DOC (f_t). To derive the propagation of measurement

431 uncertainty from equation (17) in **Supplementary Methods**, we set $c_{1X} = 2.1\%$, $c_{5X} =$

432 4.1%, $p_l = 12.5\%$, $p_c = 12.5\%$ as standard values and calculate the measurement

433 uncertainty of FT-ICR-MS (σ_m) using the replicates (see **Supplementary Methods**).

434

Parameter	Estimation (%)	Propagation uncertainty (%)
Exp. O		
c_l	54.9	3.3
c_c	25.2	3.4
f_l	4.4	0.3
f_c	9.1	1.2
f_t	86.6	1.2
Exp. P		
c_l	47.8	3.2
c_c	21.9	4.6
f_l	5.0	0.3
f_c	10.5	2.2
f_t	84.5	2.2

435

436 **Table 3.** Sensitivity analysis for each parameter in estimating the percentage of

437 $RDOC_t$ in SPE DOC (f_t).

438

Parameter	Standard Value (%)	Parameter range (%)	f_t range (%)
Exp. O			
c_l	54.9	51.6~58.1[a]	86.3~86.9
c_c	25.2	21.9~28.6	85.2~87.6
c_{1X}	2.1	1.4~2.8	84.6~88.5
c_{5X}	4.1	2.6~5.6	78.8~93.2
p_l	12.5	0.0~25.0	85.9~87.1
p_c	12.5	0.0~25.0	85.0~87.7
Exp. P			
c_l	47.8	44.6~51.0	84.2~84.8
c_c	21.9	17.3~26.5	81.7~86.3
c_{1X}	2.1	1.4~2.8	82.6~86.5
c_{5X}	4.1	2.6~5.6	76.3~91.9
p_l	12.5	0.0~25.0	83.7~85.1
p_c	12.5	0.0~25.0	82.7~85.8

439 [a]: the ranges of parameter c_l and c_c are set to be one standard deviation (calculated
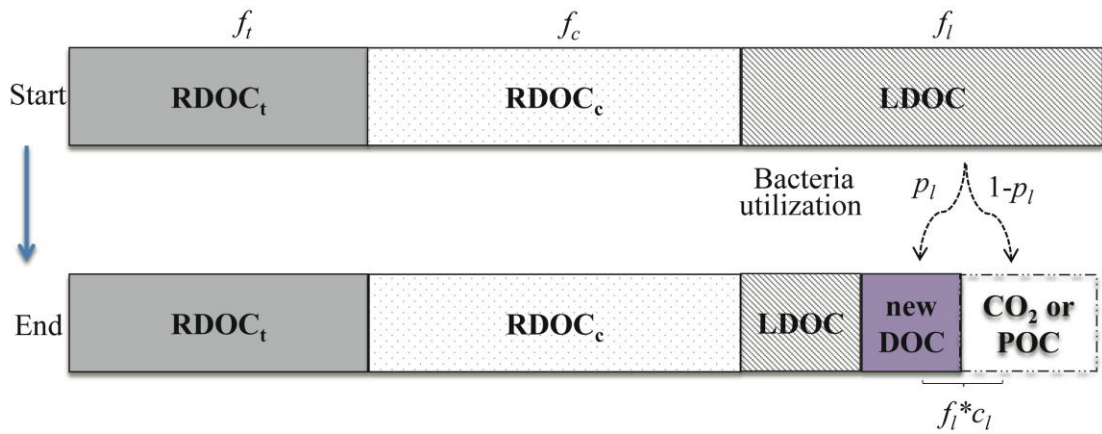440 from the propagation uncertainty analysis) away from their mean values.

Figure Legends

Figure 1. Schematic representation of the transformation of deep oceanic DOC components in incubation experiments with different DOC concentration treatments. The SPE DOC in the deep ocean is composed of structurally recalcitrant $RDOC_t$, recalcitrant DOC due to dilution ($RDOC_c$) and labile DOC ready for microbial utilization (LDOC). The natural bacterial communities collected in the deep ocean are exposed to ambient and 5-fold concentrations of natural DOC collected from their original locations. (A) In controls, a fraction of LDOC is consumed by bacteria to generate new DOC and respire back to CO_2 or assimilate to POC. Both $RDOC_c$ and $RDOC_t$ are not consumed during this process. (B) In the 5-fold concentrated treatments, except the LDOC, a fraction of $RDOC_c$ components whose concentrations become sufficient for microbial utilization are also utilized and contribute to the SPE DOC decrease. Detailed description of symbols can be seen in Table1.

Figure 2. Expected DOC utilization as a function of DOC enrichment when the RDOC is composed of intrinsically labile DOC (LDOC and $RDOC_c$) and $RDOC_t$. The simulation is the same as in Arrieta et al. (Arrieta et al., 2015a) but assumes that 0% (A), 10% (B), 50% (C), and 90% (D) of RDOC is $RDOC_t$. The 40-day time is denoted as a dotted line. The result of (A) is the same as Figure 1B in Arrieta et al. (Arrieta et al., 2015a) assuming that the DOC utilization is solely limited by concentration. Detailed simulation can be seen in Supplementary Methods.
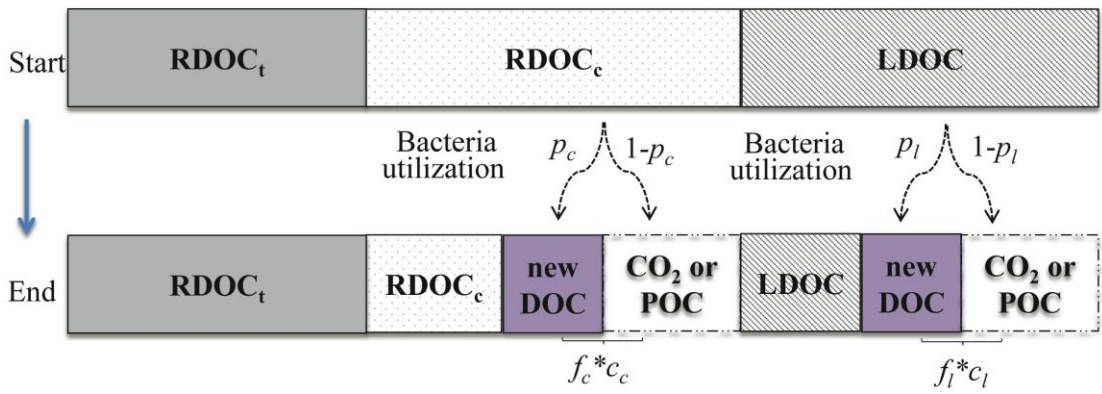
Figure 3. Two possible interpretations for the small proportion of SPE DOC consumption in a 40-day incubation. (A) A large fraction of the SPE DOC is intrinsically labile and complete consumption of it would take a long time. This is what has been proposed in Arrieta et al. (2015a). (B) According to our estimates, there is a small amount of intrinsically labile DOC in the SPE DOC and it is rapidly utilized.
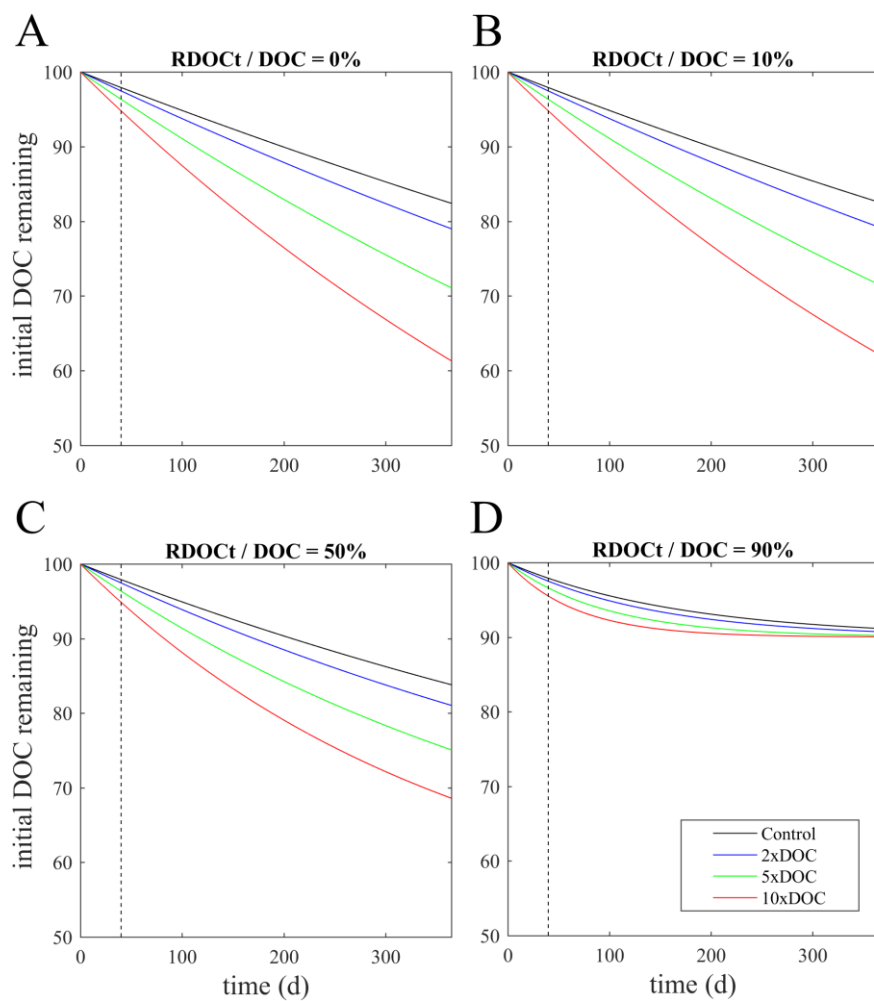
466   **Figure 1.**

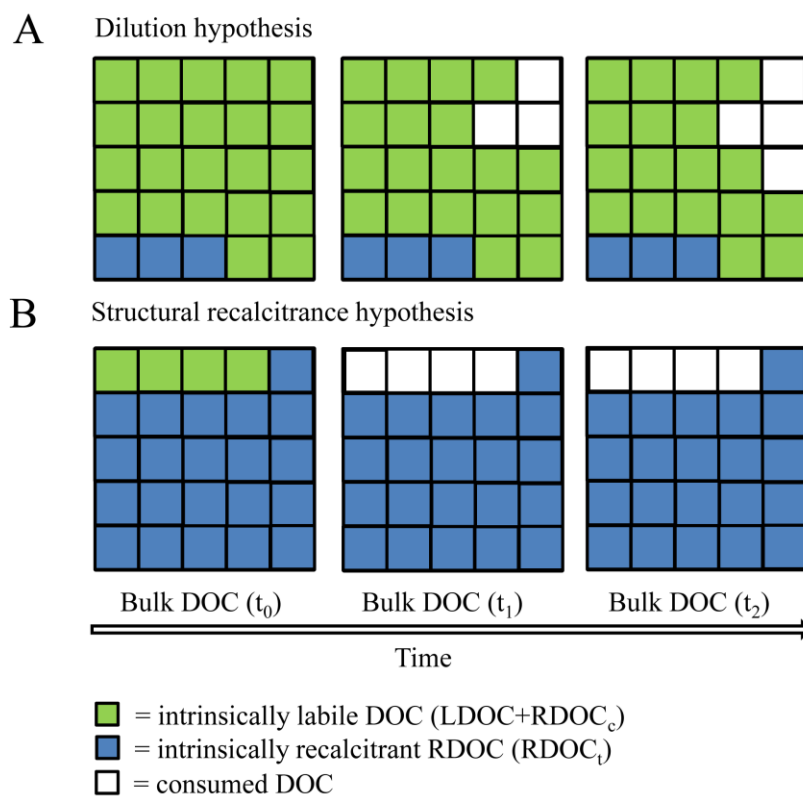## A) Controls

B) 5-fold concentration experiments

467

468   **Figure 2.**

469

470

Figure 3.

A   Dilution hypothesis

B   Structural recalcitrance hypothesis

Bulk DOC (t_0)   Bulk DOC (t_1)   Bulk DOC (t_2)

Time

◼ = intrinsically labile DOC (LDOC+RDOC$_c$)
◼ = intrinsically recalcitrant RDOC (RDOC$_t$)
☐ = consumed DOC

Supplementary Methods

Data description

The dataset (http://digital.csic.es/handle/10261/111563) used in this study is taken from DOC enrichment experiments (Arrieta et al., 2015a), in which the dilution hypothesis was tested against whether bacterial growth increased with increasing DOC concentrations. The FT-ICR-MS fingerprints of SPE DOC at the beginning and at the end of the experiments in controls (1X DOC) and in concentrated samples (5X DOC) were also collected, which allow us to investigate the degradation of thousands of different molecules simultaneously. The FT-ICR-MS datasets, together with the change of SPE DOC concentrations, are used in our study.

Model description

As shown in the conceptual model (**Figure 1**), DOC is assumed to be composed of structurally recalcitrant DOC ($RDOC_t$), recalcitrant DOC due to dilution ($RDOC_c$) and labile DOC ready for microbial utilization (LDOC), with their percentage in DOC pool being f_t, f_c, and f_l, respectively (see **Table 1** for details of variable indicators). Here, LDOC compounds are labile, whose concentrations are above the corresponding microbial uptake thresholds in both controls and 5-fold concentrated treatments. $RDOC_c$ compounds are also intrinsically labile, but their concentrations are below the corresponding uptake thresholds in controls and above those in 5-fold concentrated treatments. We have

$$f_t + f_c + f_l = 1. \tag{1}$$

In controls, only LDOC is utilized, while $RDOC_c$ is not utilized because its concentration is below the microbial uptake thresholds. A fraction of LDOC consumed by bacteria is regenerated to new DOC with the ratio of the regenerated DOC to consumed LDOC being p_l. The rest, i.e., $1 - p_l$ of consumed LDOC, is respired to CO_2 or assimilated to POC. The remaining components from $RDOC_c$ and $RDOC_t$ pools are not utilized either because of the dilution limit (i.e., $RDOC_c$) or structurally recalcitrance (i.e., $RDOC_t$). The process describing transformation of DOC components in controls can be represented as follows:

$$f_t + f_c + f_l(1 - c_l) + f_l c_l p_l = 1 - c_{1X}, \qquad (2)$$

where c_{1X} denotes the percentage of consumed DOC in relation to SPE DOC in controls and c_l represents the ratio of consumed LDOC to bulk LDOC. By subtracting equation (2) from (1), we have following equation for controls:

$$f_l c_l(1 - p_l) = c_{1X}. \qquad (3)$$

In 5-fold concentrated treatments, a fraction of $RDOC_c$ compounds become bioavailable because their concentrations are high enough to support the bacterial metabolism. Therefore, except for the consumption of LDOC, which is supposed to be the same as that in controls, $RDOC_c$ is also utilized. Therefore, for 5-fold concentrated treatments,

$$f_t + f_c(1 - c_c) + f_c c_c p_c + f_l(1 - c_l) + f_l c_l p_l = 1 - c_{5X}, \qquad (4)$$

where c_{5X} denotes the percentage of consumed DOC in relation to SPE DOC in 5-fold concentrated treatments, c_c represents the ratio of consumed $RDOC_c$ to bulk $RDOC_c$, and p_c is the new DOC produced per unit of $RDOC_c$ consumed. By subtracting equation (4) from (2), we have

$$f_c c_c (1 - p_c) = c_{5X} - c_{1X}. \tag{5}$$

41 Equations (3) and (5) explicitly link the degradation of LDOC and $RDOC_c$

42 components with the SPE DOC utilization. Then f_l and f_c can be derived from these

43 two equations:

$$f_l = \frac{c_{1X}}{c_l (1 - p_l)}. \tag{6}$$

$$f_c = \frac{c_{5X} - c_{1X}}{c_c (1 - p_c)}. \tag{7}$$

44 Finally, the percentage of $RDOC_t$ in SPE DOC can be estimated from equation (1) as:

45

$$f_t = 1 - \frac{c_{1X}}{c_l (1 - p_l)} - \frac{c_{5X} - c_{1X}}{c_c (1 - p_c)}. \tag{8}$$

46 The required parameters, i.e., c_{1X}, c_{5X}, p_c, p_l, c_c, and c_l, are estimated in the following

47 section.

Parameter estimation

49 *c_l and c_c*: Following the idea proposed by Arrieta and coworkers, a utilization index is

50 derived from FT-ICR-MS data, which is defined by subtracting the remaining relative

51 contribution at the end of controls from the initial relative contribution for each mass

52 peak, as follows

$$I^l = \frac{H^0 - (1 - c_{1X}) H^{1X}}{H^0}, \tag{9}$$

53 where H^0 and H^{1X} are the normalized FT-ICR-MS signal of SPE DOC at the

54 beginning and at the end of controls, respectively. The term $(1 - c_{1X}) H^{1X}$ can be

55 interpreted as the DOC normalized relative peak magnitude (Lechtenfeld et al., 2014).

A positive I^l indicates the net utilization (bacterial usage minus regeneration) of the corresponding intrinsically labile compound. When I^l is negative, it means that the regeneration of this compound is more than its consumption. As a result, I^l provides the lower boundary of the compound production but no information about the decrease of this compound. Therefore, c_l is estimated by averaging the utilization index I^l on molecules whose index values are positive, i.e.,

$$c_l > c_l^* = \frac{1}{N_l} \sum_{I^l > 0} I^l, \tag{10}$$

where N_l denotes the number of molecules whose index values is positive.

Compared with controls, a fraction of $RDOC_c$ compounds are utilized in 5-fold concentrated treatments and the consumption of LDOC is supported to be the same. Thus, we can also identify the utilization index of $RDOC_c$ by comparing the relative contribution of FT-ICR-MS at the end of controls and 5-fold concentrated treatments:

$$I^c = \frac{(1 - c_{1X})H^{1X} - (1 - c_{5X})H^{5X}}{(1 - c_{1X})H^{1X}}, \tag{11}$$

where H^{5X} is the normalized FT-ICR-MS signal of SPE DOC at the end of 5-fold concentrated treatments. Let N_c be the number of mass peaks with positive values of I^c, we calculate c_c as

$$c_c > c_c^* = \frac{1}{N_c} \sum_{I^c > 0} I^c. \tag{12}$$

The terms c_l^* and c_c^* in equations (10) and (12) could possibly provide the lower limits of c_l and c_c. This is because 1) the defined utilization index (i.e., I^l and I^c) calculates the proportion of consumed labile DOC to SPE DOC, which would be smaller than the ratio of consumed labile DOC to labile DOC (i.e., c_l and c_c); 2) due to

74   the dynamical transformation process of DOC, the observed utilization index actually

75   represents a net decrease of intrinsically labile compounds that subtract the DOC

76   regeneration from its consumption.

77   c_{1X} *and* c_{5X}**:** Because no DOC consumption data are reported for Stations O and P

78   (Arrieta et al., 2015a), the DOC consumption information from Stations K, L, and N

79   are used as the proxies of that for both Stations O and P. The DOC consumption data

80   from Station M is excluded because they are anomalous due to the observation of a

81   second phase of intense growth (Arrieta et al., 2015a). The percentage of consumed

82   SPE DOC is approximated to be 2.1±0.7% for c_{1X} (average ± SE) and 4.1±1.5% for

83   c_{5X} (average ± SE).

84   p_c *and* p_l**:** A portion of intrinsically labile DOC consumed by bacteria is converted

85   into bacterial-derived DOC, representing approximately 25% of the respired carbon

86   (Stoderegger and Herndl, 1998). Considering that the bacterial respired carbon

87   amounts to approximately 35.0% ~ 99.0% of the assimilated organic carbon (Del

88   Giorgio and Cole, 1998), we have the ranges of the newly produced DOC per unit of

89   LDOC or $RDOC_c$ consumed from 0.0% to 25.0%, and set the mean value of their

90   range (i.e., 12.5%) as their standard value. The bacterial-derived DOC can be

91   progressively used during the incubation, which leads to an even lower amount of

92   newly produced DOC per unit of consumed intrinsic DOC in reality.

93   **Error propagation analysis**

94   Uncertainty propagation for f_l, f_c and f_t derived from the measurement variability of

95   FT-ICR-MS fingerprints of SPE DOC is estimated as follows. Except for the controls

96   at the beginning of the experiments, each scenario has two or three replicates for the

97   FT-ICR-MS fingerprints of SPE DOC. We first obtain the distribution of measurement

98   variability by assembling the standard deviation of intensity for each molecule across

99   all scenarios and determine its 95% confidence level as the measurement variability

100   σ_m. The confidence level is chosen to allow us to investigate an exaggerated

101   uncertainty of measurement variability on the estimation of f_t. Applying the error

102   propagation formula, which is the function of measurement variability (Glover et al.,

103   2011), to equation (10):

$$\sigma^2(c_l) = \frac{1}{N_l^2} \sum_{I^l > 0} (1 - I^l)^2 \left\{ \frac{\sigma^2(H^{1X})}{(H^{1X})^2} + \frac{\sigma^2(H^0)}{(H^0)^2} \right\} \tag{13}$$

104   Based on equation (6), the error for f_l propagated from the c_l is estimated as

$$\sigma^2(f_l) = \left(\frac{c_{1X}}{1 - p_l} \right)^2 \frac{1}{c_l^4} \sigma^2(c_l). \tag{14}$$

105   Assuming that all molecules share the same measurement variability, i.e., $\sigma_m^2 =$

106   $\sigma^2(H^{1X}) = \sigma^2(H^0)$, by plugging equation (13) into equation (14), we have

$$\sigma^2(f_l) = \left(\frac{c_{1X}}{1 - p_l} \right)^2 \frac{\sigma_m^2}{N_l^2 c_l^4} \sum_{I^l > 0} (1 - I^l)^2 \left\{ \frac{1}{(H^{1X})^2} + \frac{1}{(H^0)^2} \right\}. \tag{15}$$

107   Similarly, the error for f_c propagated from the FT-ICR-MS fingerprints of SPE DOC is

108   estimated as

$$\sigma^2(f_c) = \left(\frac{c_{5X} - c_{1X}}{1 - p_c} \right)^2 \frac{\sigma_m^2}{N_c^2 c_c^4} \sum_{I^c > 0} (1 - I^c)^2 \left\{ \frac{1}{(H^{5X})^2} + \frac{1}{(H^{1X})^2} \right\}. \tag{16}$$

109   With the simplistic assumption that the error propagations of f_l and f_c are independent,

110   the error propagation of f_t could be represented as

$$\sigma^2(f_t) = \sigma^2(f_l) + \sigma^2(f_c). \tag{17}$$

111   **Sensitivity analysis**

112   Analyses are conducted to investigate the sensitivity of f_t to each parameter over wide

113   ranges. Six parameters in equation (8) are considered. Specifically, the ranges of c_l

114   and c_c are set to be one standard deviation, which is calculated from the error

115   propagation analysis, away from their base values. The ranges of c_{1X} and c_{5X} are set to

116   be one standard deviation away from their base values as well. Both p_l and p_c are

117   varied from 0.0% to 25.0% to cover most likely range.

118   **Calculate the consumption of SPE DOC as a function of DOC enrichment**

119   In these simulations, we explore how the utilization rate of SPE DOC changes as a

120   function of DOC enrichment given that DOC is composed of intrinsically labile DOC

121   (LDOC and $RDOC_c$) and $RDOC_t$. Our simulation is based on the simplification that

122   all components in the $RDOC_c$ pool are available for microbial utilization in

123   concentrated experiments, which could possibly lead to overestimation of the SPE

124   DOC utilization rate. Consistent with simulations in Arrieta et al. (2015b), we

125   consider four different DOC concentration levels (controls and the corresponding

126   two-, five- and ten-fold concentrations of nature DOC). Let $x(t)$ be the concentration

127   of intrinsically labile compounds at day t. Assuming that the utilization rate is a

128   function of concentration and cell abundance, we have

$$\frac{dx(t)}{dt} = x(t)K_s S, \tag{18}$$

129   in which K_s is the Monod substrate affinity constant and S the maximum cell

130   abundances observed in the experiment. The solution of equation (18) can be

131   represented as:

$$x(t) = x(0)e^{-K_s St}. \tag{19}$$

132   Let $z(0)$ be the initial DOC concentration:

$$x(t) = z(0)\gamma e^{-K_s S t}, \qquad (20)$$

133   in which $\gamma = f_l + f_c$. $z(0)$ is set to 30 (in arbitrary units), and the cell abundances S for

134   controls, two-, five- and ten-fold concentration treatments are 55, 67, 97, and 139

135    $\times 10^6$ prokaryotes L^{-1}, respectively (Arrieta et al., 2015b). The substrate affinity

136   constant S is calculated by reconciling the proportion of consumed SPE DOC at $t = 40$

137   in equation (20) to that of the observed values in the controls (i.e., c_{1X}). Therefore,

$$K_s = \frac{\ln (1 - c_{1X}/\gamma)}{-40 \times 55 \times 10^6}. \qquad (21)$$

138   By plugging (21) into (20), the proportion of consumed SPE DOC at t day is given as:

$$c(t) = \frac{x(t) - x(0)}{z(0)} = \gamma(e^{-K_s S t} - 1). \qquad (22)$$

139   In our simulation, γ ranges from 0 to 1. All SPE DOC is RDOC$_t$ when $\gamma = 0$ and is

140   RDOC$_c$/LDOC when $\gamma = 1$. We also conducted sensitivity analysis to investigate the

141   change of $c(t)$ by varying c_{1X} from 1.4% to 2.8% in equation (21).

142   **Reference**

143   Arrieta, J.M., Mayol, E., Hansman, R.L., Herndl, G.J., Dittmar, T., and Duarte, C.M. (2015a) Dilution
144   limits dissolved organic carbon utilization in the deep ocean. *Science* **348**: 331-333.

145   Arrieta, J.M., Mayol, E., Hansman, R.L., Herndl, G.J., Dittmar, T., and Duarte, C.M. (2015b) Response
146   to Comment on "Dilution limits dissolved organic carbon utilization in the deep ocean". *Science*
147   **350**: 1483-1483.

148   Del Giorgio, P.A., and Cole, J.J. (1998) Bacterial growth efficiency in natural aquatic systems.
149   *Annual Review of Ecology and Systematics* **29**: 503-541.

150   Glover, D.M., Jenkins, W.J., and Doney, S.C. (2011) *Modeling methods for marine science*: Cambridge
151   University Press.

152   Lechtenfeld, O.J., Kattner, G., Flerus, R., McCallister, S.L., Schmitt-Kopplin, P., and Koch, B.P. (2014)
153   Molecular transformation and degradation of refractory dissolved organic matter in the
154   Atlantic and Southern Ocean. *Geochimica et Cosmochimica Acta* **126**: 321-337.

155   Stoderegger, K., and Herndl, G.J. (1998) Production and release of bacterial capsular material and
156   its subsequent utilization by marine bacterioplankton. *Limnology and Oceanography* **43**: 877-
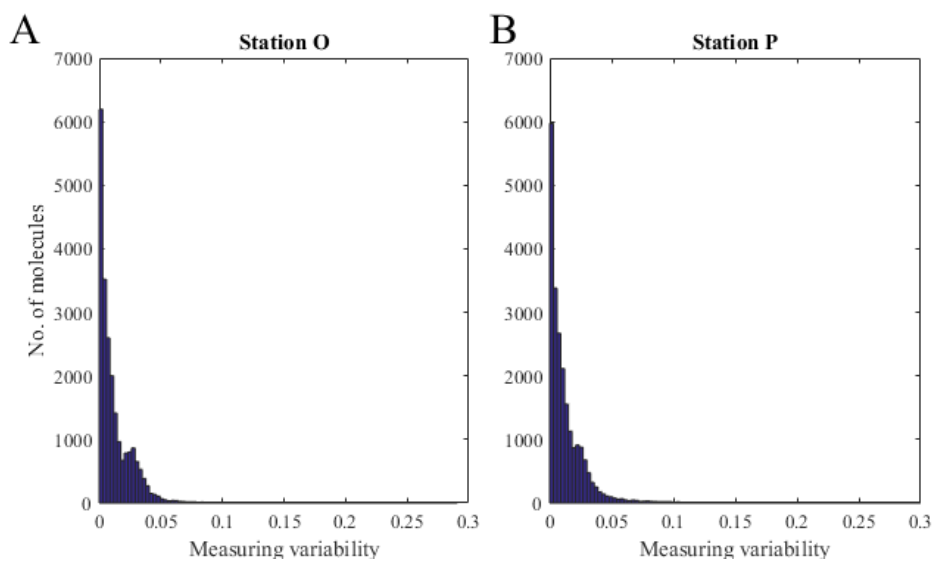157   884.

158

Supplementary Tables

Table S1. Matrix effect on estimating the percentage of $RDOC_t$ in SPE DOC (f_t). Here, we consider the matrix effect caused by the incubation process (i.e., change of signal intensity from DOC component during incubation experiments) and concentrated treatments (i.e., change of signal intensity due to DOC concentrated treatments). The measurement uncertainty caused by matrix effect (i.e., σ_{ME}) is calculated as the 95th percentile of signal intensity difference by comparing 1X initial and 1X final FT-ICR-MS, 1X initial and 5X initial FT-ICR-MS, 5X initial and 5X final FT-ICR-MS, respectively. We then investigate the matrix effect on the estimation of f_t according to equation (17) in Supplementary Methods.
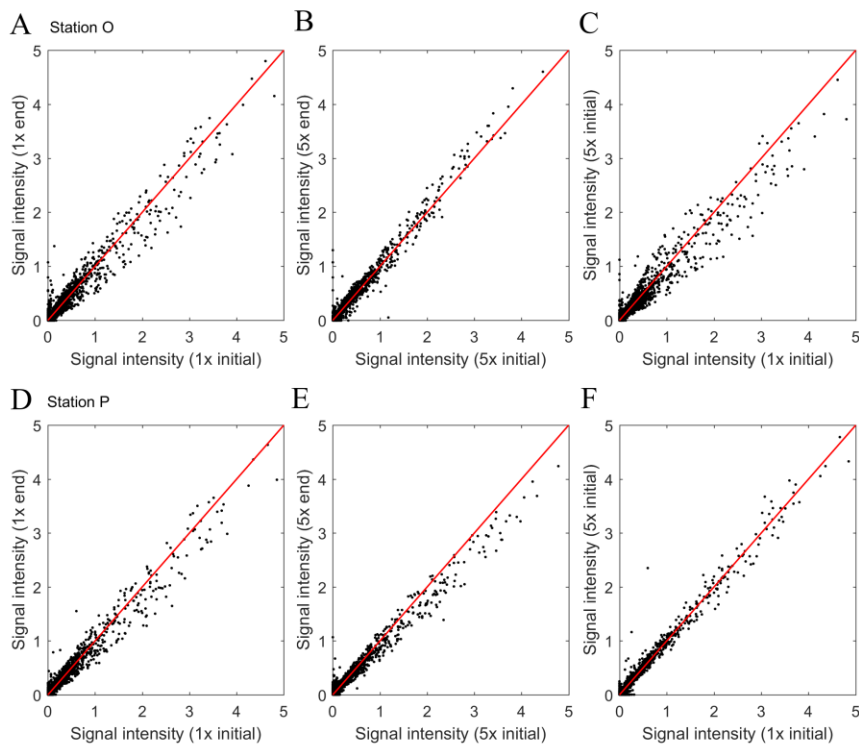
		Exp. O	Exp. P
σ_{ME}	1X initial, 1X final	0.084	0.073
	1X initial, 5X initial	0.074	0.040
	5X initial, 5X final	0.066	0.068
Max. of σ_{ME}		0.084	0.073
Range of f_t, %		82.1~89.1	77.8~87.9

Supplementary Figures

Figure S1. Histogram distribution of measurement variability of FT-ICR-MS fingerprints of DOC by assembling all molecules together. The measurement variability for each molecule is calculated as the standard deviation of its relative intensities from replicates. The average measurement variability FT-ICR-MS (i.e., σ_m) is chosen as the 95th percentile of this distribution for the downstream propagation uncertainty analysis.

Figure S2. Comparison of signal intensity of FT-ICR-MS to assess DOC composition change during the incubation experiments (A, B, D, E) and the matrix effect due to DOC concentrated treatments (C, F). The diagonal line is shown in the red color in each figure. The close to the diagonal line means that the overall FT-ICR-MS signal pattern is similar among different treatments.